Large area self-assembled masking for photonic applications

N. Nagy,[a] A. E. Pap, E. Horváth, J. Volk,[b] and I. Bársony[c]
Research Institute for Technical Physics and Materials Science (MFA), MTA, H-1525 Budapest, Hungary

A. Deák and Z. Hórvölgyi
Department of Physical Chemistry, Budapest University of Technology and Economics, H-1521 Budapest, Hungary

(Received 10 April 2006; accepted 26 June 2006; published online 8 August 2006)

Ordered porous structures for photonic application were fabricated on *p*- and *n*-type silicon by means of masking against ion implantation with Langmuir-Blodgett (LB) films. LB films from Stöber silica spheres [J. Colloid Interface Sci. **26**, 62 (1968)] of 350 nm diameter were applied in the boron and phosphorus ion-implantation step, thereby offering a laterally periodic doping pattern. Ordered porous silicon structures were obtained after performing an anodic etch and were then removed by alkaline etching resulting in the required two-dimensional photonic arrangement. The LB silica masks and the resulting silicon structures were studied by field emission scanning electron microscope analysis. © *2006 American Institute of Physics*. [DOI: 10.1063/1.2335668]

Photonic structures, such as photonic crystals and structures utilizing surface plasmon effects, all require the preparation of high resolution, periodic masking patterns on a large area. Self-assembly of nanospheres offers an inexpensive masking alternative with a wide range of control over area and dot size. A number of recent publications deal with photonic crystal[1] realizations and laboratory-on-chip[2] applications based on ordered micro- and macroporous silicon structures. In order to fabricate ordered structures by anodization, however, a prepatterning of the large surface is needed, but in the submicrometer region the resolution of conventional photolithography is insufficient. Possible alternative options are electron beam lithography,[3] holography,[4,5] fast ion beam[6] etching, or optical lithography combined with silylation.[7] High resolution periodic patterning, however, can be obtained relatively simply by means of using inexpensive self-assembled nanoparticles. In the case of porous silicon they can be used as a masking layer for the ion-implantation step to provide the laterally periodic doping pattern.

The Langmuir-Blodgett (LB) technique is commonly used to prepare molecular films on solid supports.[8] Recently, it has also been applied to the deposition of micro- and nanoparticulate films. The LB method enables us to transfer the structure, previously formed in a film balance at liquid-air interface, onto a solid support such as a silicon wafer.

Stöber's method[9] has been used for several decades to prepare silica nanoparticles in a wide size range by the controlled hydrolysis of tetra-alkyl orthosilicates.[10] These particles have the advantageous properties above diameters of ca. 20 nm (Ref. 11) of nearly spherical shape and narrow size distribution.

In this work we demonstrate the use, for photonic crystal applications, of self-assemble nanosphere lithography[12] for the formation of ordered porous patterns of submicrometer period. The self-assembled film serves as a masking layer for ion implantation which in turn generates the periodically inhomogeneous doping for the subsequent anodization step.

The alcosol of the silica particles was prepared according to Stöber's method[13] by controlled hydrolysis of tetraethyl orthosilicate. The diameter of prepared silica particles was 350 nm with standard deviation ca. 10%, obtained from transmission electron microscopy (TEM) analysis.

Layer deposition was carried out on 25×25 mm^2 rectangular silicon substrates, previously cleaned in a 2% HF solution, and rinsed by de-ionized water and absolute ethanol, and finally dried at room temperature.

To prepare the Langmuir films of nanoparticles we used a laboratory-built Wilhelmy film balance. The alcosols were diluted by chloroform at a volume ratio of 1:2. The sol samples were homogenized—prior to spreading—for 10 min in an ultrasonic bath. The substrate was first immersed into the water; then the appropriate amount of the sol was spread onto the water surface in the film balance at (23 ± 1) °C. After evaporation of the spreading liquid (in ca. 5 min) the layer was compressed at a rate of 33 cm^2/min. The surface pressure of the layer was monitored with the Wilhelmy-plate method. At ca. 80% of the collapse pressure of the sample,

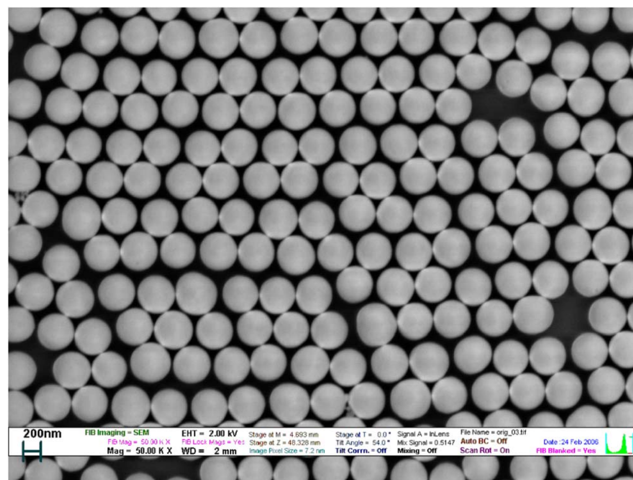

FIG. 1. FESEM image of the monolayer silica LB film used as the masking layer during ion implantation.

[a]Electronic mail: nagyn@mfa.kfki.hu

[b]Present address: International Center for Young Scientists (ICYS), National Institute for Materials Science (NIMS), 1-1 Namiki, Tsukuba, Ibaraki 305-0044, Japan.

[c]Also of the Department of Nanotechnology, Pannon University, H-8200 Veszprém, Hungary.

 © 2006 American Institute of Physics
Downloaded 06 May 2008 to 148.6.76.162. Redistribution subject to AIP license or copyright; see http://apl.aip.org/apl/copyright.jsp

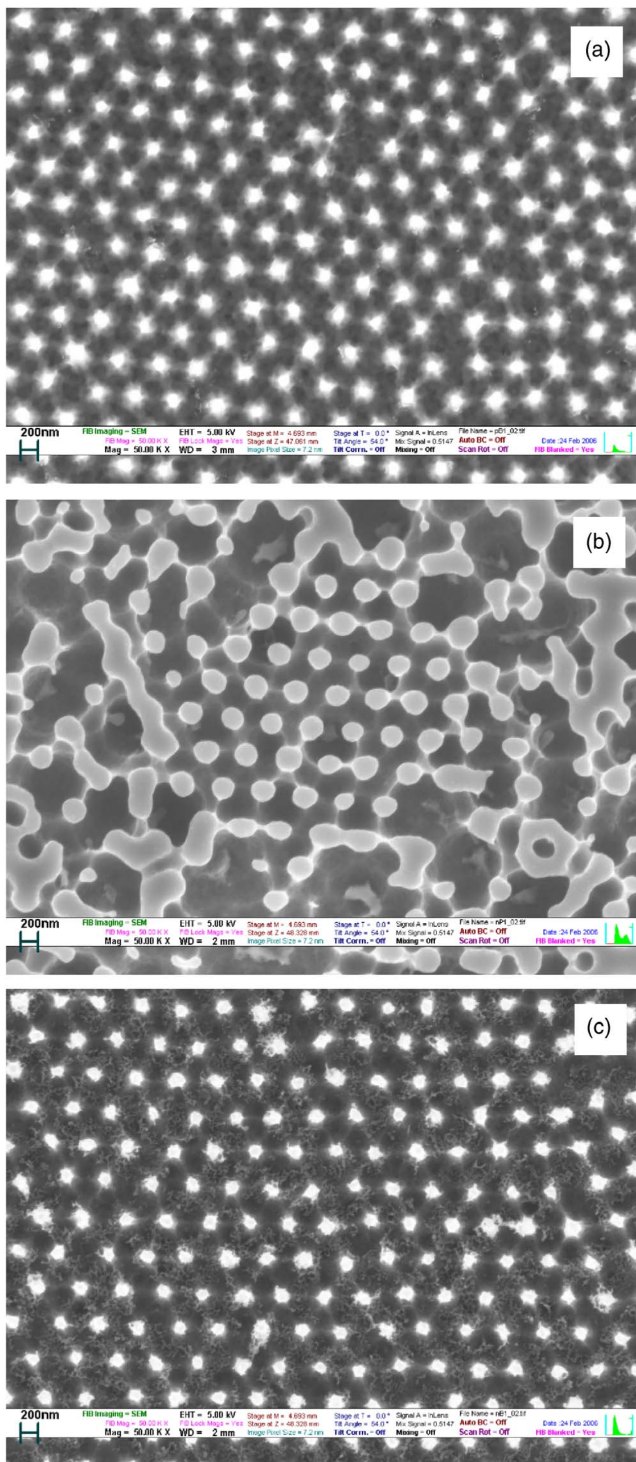

FIG. 2. FESEM images of the B^+-implanted *p*-type sample (a), the P^+-implanted *n*-type sample (b), and the B^+-implanted *n*-type sample (c) after removal of the porous layer. Etching occurred preferably in the implanted regions between the nanospheres, where the ions penetrated the substrate.

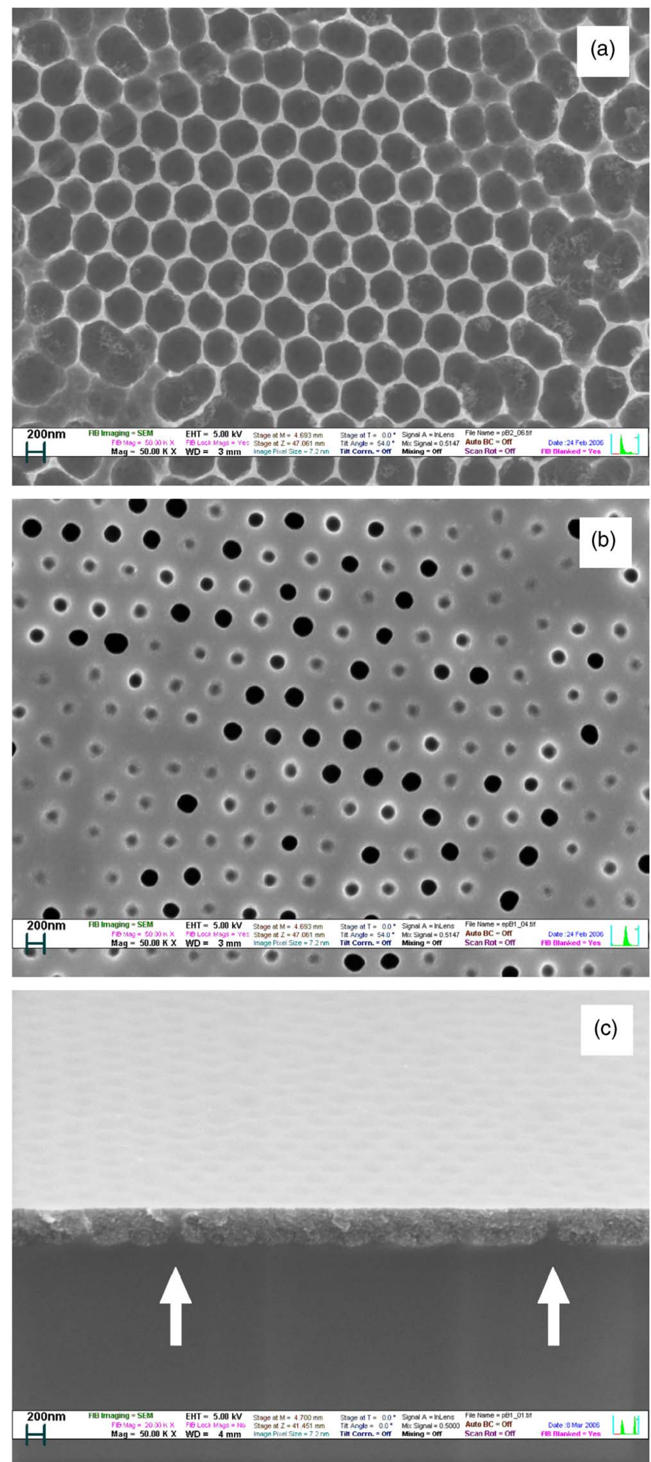

FIG. 3. FESEM image of the B^+-implanted *p*-type sample, through a double-layered LB masking film: (a) The honeycomblike pore structure after removal of the porous layer originated from the lateral protrusion of the circular pores during anodization. (b) FESEM image of the P^+-implanted *p*-type sample after removal of the porous layer. It was etched in the nonimplanted regions in the area underneath the nanoparticles, i.e., masked by the nanospheres. (c) Cross-section FESEM image of the B^+-implanted *p*-type sample [see Fig. 2(a)] before removal of the PS layer. On the cleaved cross section two of the crystalline silicon pillars are marked.

the immersed silicon substrate was educed from the water vertically at a constant surface pressure, and the film dried for 10 min under a 50 W halogen lamp.

These monolayer (Fig. 1) and one double-layer LB silica films were deposited on (100) oriented *p*-type (10–15 Ω cm) and *n*-type (4–6 Ω cm) silicon wafers as mask for the 10^{14} ions/cm^2 boron and phosphorus implantations at 20 keV. After ion implantation the LB silica films were removed mechanically prior to the thermal annealing of the samples, which was carried out at 600 °C for 30 min and at 900 °C for 60 min, respectively.

The electrochemical etching of the B^+- and P^+-implanted *p*- and *n*-type silicon substrates was carried out in a 7:3 HF:ethanol electrolyte. The controlled current density was 25 mA/cm^2 for all samples. The duration of anodization was

Downloaded 06 May 2008 to 148.6.76.162. Redistribution subject to AIP license or copyright; see http://apl.aip.org/apl/copyright.jsp

12 s for the *p*-type and 14 s for the *n*-type wafers. For the B^+- and P^+-implanted *n*-type silicon samples, the electrochemical etching was performed with front side illumination by a 100 W halogen lamp. It is worth noting that in the case of *n*-type wafers the silicon etching started only after the illumination was turned on.

Monitoring of the evolution of ordered porous structures was afforded by the diffraction of light which was immediately observable with the naked eye for each sample after the anodization step. The porous silicon (PS) layers were then removed by alkaline etch for field emission scanning electron microscopy (FESEM) analysis with a LEO 1540 XB microscope.

In both starting materials, the *p*-type silicon wafer of 10–15 Ω cm and the *n*-type wafer of 4–6 Ω cm resistivity, the order of magnitude of the doping density is 10^{15} cm^{-3}. According to Monte Carlo simulations (SRIM 2003) the magnitude of the doping concentration in the volume affected by the implantation is 10^{19} cm^{-3}. The depth of the B^+-implanted layer is ca. 120 nm (ion range: 80 nm, straggle: 32 nm) and that of the P^+-implanted is ca. 50 nm (ion range: 31 nm, straggle: 14 nm). The implanted B^+ and P^+ ions certainly cannot penetrate the masking layers formed by the nanospheres, due to their characteristic depths of 200 and 90 nm SiO_2, respectively.

Therefore, in the case of B^+-implanted *p*-type [Fig. 2(a)], P^+-implanted *n*-type [Fig. 2(b)] and B^+-implanted, *n*-type [Fig. 2(c)] silicon, the samples were preferably anodized in the implanted regions between the nanospheres. The evidence for this can be found in Fig. 2(a). The crystalline silicon pillars (bright spots in the plain view) are missing wherever there was a nanosphere vacancy in the LB masking layer (see Fig. 1).

Figure 2(b) shows that the patterns are periodic over an area of diameter >4 μm on the surface of the P^+-implanted *n*-type sample. These regions were separated by defected regions of similar size occurring regularly over the whole masked surface area.

In the case of the B^+-implanted *n*-type sample [Fig. 2(c)] the porous etching occurred preferentially between the silica particles, where the B ion implantation determined the type of doping (i.e., by changing the doping polarity by overcompensation). Similarly to Fig. 2(a) this figure shows that the crystalline silicon pillars are missing in the matrix points, wherever a nanosphere vacancy was formed in the LB masking layer.

In the case of the double-layer masked sample the B^+ ions could reach the substrate, owing to the geometry of tetrahedral ordering of the spheres in the close packed structure, through nearly circular windows of diameter ca. only 60 nm. The faveolate (honeycomblike) pore structure in Fig. 3(a) is the result of the lateral extension of the porous etching from the circular implantation-doped regions during anodization. The anodic etching stops upon depletion of holes in the bordering region separating the porous spots. This is the result of a sensitive balance between the actual diffusion lengths of holes and the local depth of the porous regions in the substrate. These periodic patterns in an area of diameter >4 μm were again separated by defected regions of similar size, but occurred regularly on the whole masked surface, similarly to the P^+-implanted *n*-type sample.

The P^+-implanted *p*-type sample [Fig. 3(b)] was, however, etched just underneath the nanoparticles, i.e., in the regions masked by the nanospheres against the opposite doping. Traces of imperfections in the original LB layer can also be seen here.

The thickness of the anodized PS layer was found from cross-section FESEM analysis to be ca. 400–450 nm for the *p*-type samples and 500–550 nm for the *n*-type samples. The ordered structure can also be found in the etched volume of the *p*-type samples [Fig. 3(c)].

Recent advances in alignment control of mesoporous silica films[14] open up the possibility of uniform coating over large, even wafer-size, areas free of grain boundary defects.

This work was supported by grants from the Hungarian Foundation for Scientific Research, OTKA Nos. T 046696 and T 049156, and from the Hungarian National Office for Research and Technology in the NKFP Project 3A/079/2004 "Aquanal." The support of Attila L. Tóth and Attila L. Kovács with SEM and TEM analyses is gratefully acknowledged.

[1] F. Muller, A. Birner, U. Gosele, V. Lehmann, S. Ottow, and H. Foll, J. Porous Mater. **7**, 201 (2000).
[2] V. S. Y. Lin, K. Motesharei, K. P. S. Dancil, M. J. Sailor, and M. R. Ghadiri, Science **278**, 840 (1997).
[3] S. Borini, S. D'Auria, M. Rossi, and A. M. Rossi, Lab Chip **5**, 1048 (2005).
[4] G. Lerondel, R. Romestain, J. C. Vial, and M. Thonissen, Appl. Phys. Lett. **71**, 196 (1997).
[5] N. Nagy, J. Volk, A. Hamori, and I. Barsony, Phys. Status Solidi A **202**, 1639 (2005).
[6] P. Schmuki, L. E. Erickson, and D. J. Lockwood, Phys. Rev. Lett. **80**, 4060 (1998).
[7] A. G. Nassiopoulos, S. Grigoropoulos, L. Canham, A. Halimaoui, I. Berbezier, E. Gogolides, and D. Papadimitriou, Thin Solid Films **255**, 329 (1995).
[8] A. Ulman, *An Introduction to Ultrathin Organic Films From Langmuir-Blodgett to Self-Assembly* (Academic, New York, 1991), p. 116.
[9] W. Stöber, A. Fink, and E. Bohn, J. Colloid Interface Sci. **26**, 62 (1968).
[10] T. Matsoukas and E. Gulari, J. Colloid Interface Sci. **124**, 252 (1988).
[11] J. K. Bailey and M. L. Mecartney, Colloids Surf. **63**, 131 (1992).
[12] J. C. Hulteen and R. P. Vanduyne, J. Vac. Sci. Technol. A **13**, 1553 (1995).
[13] Gy. Tolnai, F. Csempesz, M. Kabai-Faix, E. Kalman, Z. Keresztes, A. L. Kovacs, J. J. Ramsden, and Z. Horvolgyi, Langmuir **17**, 2683 (2001).
[14] H. Miyata, T. Suzuki, A. Fukuoka, T. Sawada, M. Watanabe, T. Noma, K. Takada, T. Mukaide, and K. Kuroda, Nat. Mater. **3**, 651 (2004).

Downloaded 06 May 2008 to 148.6.76.162. Redistribution subject to AIP license or copyright; see http://apl.aip.org/apl/copyright.jsp